

Dynamics of hydrogen bonds and vibrational spectral diffusion in liquid methanol from first principles simulations with dispersion corrected density functional



Vivek Kumar Yadav, Amalendu Chandra^{*}

Department of Chemistry, Indian Institute of Technology, Kanpur 208 016, India

ARTICLE INFO

Article history:

Received 7 November 2012

In final form 22 January 2013

Available online 4 February 2013

Keywords:

Hydrogen bond dynamics

Vibrational spectral diffusion

Methanol dynamics

Dispersion interactions

Ab initio molecular simulation

ABSTRACT

The effects of dispersion interactions on the dynamics of hydrogen bonds and vibrational spectral diffusion in liquid methanol are investigated through first principles simulations with a dispersion corrected density functional. Calculations are done at two different temperatures of 300 and 350 K and the results are compared with those of an earlier study where no such dispersion corrections were included. It is found that inclusion of dispersion interactions slightly increases the number of molecules held through non-hydrogen-bonded dispersion interactions in the neighborhood which, in turn, makes the dynamics faster. The inclusion of dispersion corrections gives rise to a faster hydrogen bond dynamics compared to the case when no such dispersion corrections are made. Also, the time scale of vibrational spectral diffusion obtained with the dispersion corrected density functional is found to be in better agreement with experiments.

© 2013 Elsevier B.V. All rights reserved.

1. Introduction

In a recent paper [1], we presented an *ab initio* molecular dynamics study of liquid methanol within density functional theory using the well-known BLYP functional [2]. The calculated dynamics of hydrogen bonds and vibrational spectral diffusion [3] in the liquid were found to be slower than the experimentally reported results at room temperature [4]. A somewhat slower dynamics of vibrational spectral diffusion was also reported earlier for liquid water with the same BLYP functional [5,6]. The extent of slowing down of molecular motion was found to be even stronger for the long-time diffusion and orientational relaxation processes in water calculated with the BLYP or other similar functionals belonging to the class of generalized gradient approximation (GGA) [7–14]. In recent years, a number of first principles studies on liquid water have concluded that the calculated slower dynamics of water with BLYP and other similar functionals arise, at least in part, from the fact that these functionals do not capture the dispersion interactions properly [15–17]. In fact, there have been a number of studies on water and also methanol in recent years which have shown the importance of incorporating dispersion interactions in describing the liquid structure and dynamics of these liquids correctly [15–20]. For water, these studies have shown that the dispersion-corrected BLYP functional significantly

improves the phase diagram, structure and dynamics of the liquid when compared with the corresponding results obtained with the pure dispersion uncorrected BLYP functional [15–18]. Similar studies on methanol have also been carried out for the phase diagram and structure [19,20] and the general conclusion has been that, for methanol also, the dispersion interactions provide improved results for the thermodynamic and structural properties. In this work, we look at the effects of dispersion interactions on the dynamics of liquid methanol through first principles simulations.

In the present study, we have carried out *ab initio* molecular dynamics simulations of liquid methanol using the dispersion corrected BLYP functional, also known as the BLYP-D functional. In this functional, the dispersion corrections are incorporated to the BLYP functional [2] empirically by using the scheme of Grimme [21,22]. The simulations have been carried out at two different temperatures of 300 and 350 K. Thus, by comparing the earlier results of Ref. [1] at 300 K, we could examine the significance of dispersion interactions in the dynamics of hydrogen bond and frequency fluctuations and, by comparing the results at 300 and 350 K for the same BLYP-D functional, we could study the temperature effects on such dynamics. The *ab initio* simulations have been carried out using the Car–Parrinello method [23] and the frequency fluctuations have been calculated using the wavelet method [24] of time series analysis. Generally, it is found that the inclusion of dispersion interactions improves the dynamics and produces results which are in closer agreement with experiments [4] than those obtained earlier with the pure BLYP functional [1].

^{*} Corresponding author. Tel.: +91 512 2597241; fax: +91 512 2597436.

E-mail address: amalen@iitk.ac.in (A. Chandra).

The rest of the Paper is organized as follows. The details of *ab initio* molecular dynamics are presented in Section 2. In Section 3, we discuss the results of the structure of methanol and also of the hydrogen bonds and vibrational frequencies. The results of the dynamics of hydrogen bond fluctuations and vibrational spectral diffusion are presented in Section 4. Finally, our conclusions are briefly summarized in Section 5.

2. *Ab initio* molecular dynamics simulations

The *ab initio* molecular dynamics simulations were carried out by using the Car–Parrinello method [23,25] and the CPMD code [26]. Our simulation systems contain 32 deuterated methanol molecules at two different temperatures of 300 and 350 K. The length of the cubic simulation box is 12.9 Å which corresponds to the experimental density of methanol at room temperature [27]. The simulation box was replicated periodically in three dimensions and the electronic structure of the extended system was represented by the Kohn–Sham (KS) [28] formulation of quantum density functional theory. The KS orbitals were represented using a plane wave basis. The core electrons were treated through Troullier–Martins [29] pseudopotentials and the plane wave expansion of the KS orbitals were truncated at 70 Ry. A fictitious mass of $\mu = 800$ a.u. was assigned to the electron orbitals and a time step of 5 a.u. (0.125 fs) was used to propagate the system dynamics. All hydrogen atoms were assigned the mass of deuterium to reduce the influence of quantum effects on the dynamical properties. Our choice of CD₃OD in place of CH₃OH ensured that electronic adiabaticity and energy conservation were maintained throughout the simulations for the chosen values of the fictitious electronic mass parameter and time step. Since the main goal of the present work was to look at the effects of dispersion interactions on the dynamics of liquid methanol, we employed the dispersion corrected BLYP-D density functional in our calculations. This functional includes dispersion corrections to the pure BLYP functional [2] as introduced by Grimme [21]. We prepared the initial configurations at both temperatures through classical molecular dynamics simulations. Subsequently, we equilibrated each system through *ab initio* molecular dynamics for 15 ps in canonical ensemble and then ran each system for another 45 ps in microcanonical ensemble for the calculations of various equilibrium and dynamical properties. After the simulation trajectories were generated, we carried out a time series analysis of the coordinates and momenta of OD bonds to calculate their stretch frequencies. Specifically, we have used the wavelet method [24] of time series analysis for this purpose. The details of this method have been discussed elsewhere for calculations of fluctuating OD bond frequencies from simulation trajectories [1,5,6,30–32].

3. Structure of methanol, hydrogen bonds and vibrational frequencies

We have looked at the effects of dispersion interactions and temperature on the structure of methanol by calculating the radial distribution functions between different pairs of atoms such as oxygen–oxygen, oxygen–hydrogen and carbon–carbon pairs. The results of these correlation functions are shown in Fig. 1. It is seen that at 300 K, the inclusion of dispersion interactions slightly increases the height of the first minimum of oxygen–oxygen correlation which means a slight enhancement of the number molecules at the boundary of the neighborhood of hydroxyl group. These molecules are held through weaker non-hydrogen-bonded dispersion interactions. The enhanced dispersion interaction also shifts the first peak of carbon–carbon correlation to a slightly shorter distance. These non-hydrogen-bonded molecules are relatively

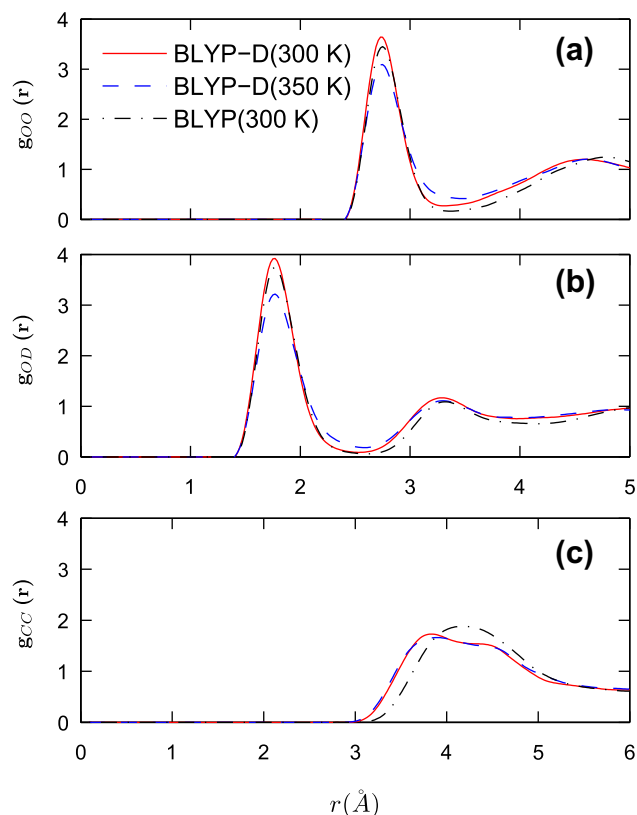


Fig. 1. The atom–atom radial distribution functions of methanol molecules. The plots of (a), (b) and (c) are for oxygen–oxygen, oxygen–hydrogen and carbon–carbon correlations. The solid and dashed curves represent the BLYP-D results at 300 and 350 K. The corresponding results for BLYP functional without dispersion corrections at 300 K, as calculated from the simulation trajectory of Ref. [1], are shown by dashed-dotted curves.

loosely held, hence increase the dynamics as discussed later in Section 4. We note that a similar, rather more pronounced, structural effect was also found for water upon inclusion of dispersion effects [15–18]. We calculated the number of hydrogen bonds per methanol molecule by integrating the corresponding oxygen–hydrogen RDF up to its first minimum. With this geometrical definition of hydrogen bonds, the average number of hydrogen bonds per methanol molecule is found to be 1.9 for BLYP-D at 300 K. The corresponding number for pure BLYP without any dispersion corrections at the same temperature is 1.95. When the temperature is raised to 350 K, peak heights of all the correlations decrease showing a reduction of structure around methanol molecules. The number of hydrogen bonds per molecule is found to be 1.82 at the elevated temperature. We note that a decrease in the hydrogen bond number with increase of temperature was also reported in an earlier *ab initio* Monte Carlo study of liquid methanol [20].

We next discuss the distributions of our calculated stretch frequencies of OD bonds. In particular, we focus on the correlations between the stretch frequencies and the hydrogen bonded structure between molecules. In Fig. 2, we have shown the contour plots of the conditional probability of observing a particular frequency for a given O–D distance for both the systems. It is clear from the contour plots that one can not assign a single instantaneous frequency to a given O–D bond because of the substantial dispersion present in the probability distributions. A comparison between Figs. 2a and 2b reveals that, at the higher temperature, the distribution is more elongated towards the longer distance. The dashed lines in these plots represent the average behavior of stretch frequencies with change of hydrogen bond distance. On average, it

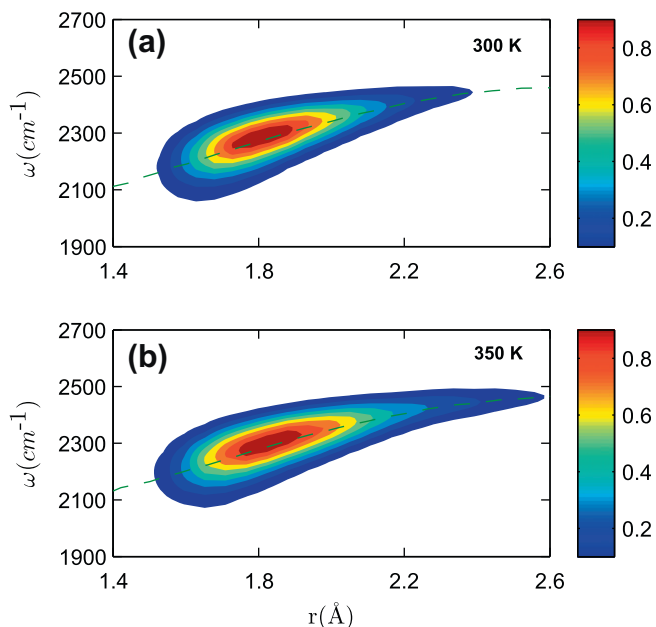


Fig. 2. The joint probability distributions of the OD frequency and D–O distance of methanol molecules at (a) 300 and (b) 350 K. The contour levels of different fractions of the maximum value are shown in different color codes.

is found that a frequency–structure correlation exists where the stretch frequency of an OD bond increases with increase of the associated D–O hydrogen bond distance. The average stretch frequencies of OD bonds of the two systems are found to be 2287 cm^{−1} and 2311 cm^{−1} at 300 and 350 K, respectively. We note that, for pure BLYP without dispersion corrections, the average frequency of methanol OD bonds at room temperature was found to be 2225 cm^{−1} [1]. Thus, there is an increase in the average frequency upon inclusion of dispersion corrections. It may be noted that for liquid water also, a slight increase in the stretch frequencies of OH bonds was reported on inclusion of dispersion corrections [15]. Also, the average frequency obtained with dispersion corrected BLYP-D is closer to the experimental frequency [4] than that found with pure BLYP [1].

4. Dynamical aspects: hydrogen bond dynamics and spectral diffusion

We first discuss the effects of dispersion interactions on the dynamics of hydrogen bonds at the two temperatures considered in this study. We have employed the so-called population correlation function approach [33–41] to look at the relaxation of hydrogen bonds in liquid methanol. We calculate the continuous probability function $S_{HB}(t)$ which is defined as the probability that an initially hydrogen bonded methanol-methanol pair remains hydrogen bonded continuously at all times up to t . The integral of this functional (τ_{HB}) gives the average lifetime of hydrogen bonds. We also calculate the intermittent probability function $C_{HB}(t)$ which gives the probability that a hydrogen bond between a pair of methanol molecules is intact at time t , given that it was intact at time zero, irrespective of possible breaking in the interim time. The decay of this intermittent probability function gives the time scales of local structural relaxation. We also calculated another intermittent probability function $N_{HB}(t)$ which gives the probability that a pair of molecules which were hydrogen bonded at $t = 0$, remains as nearest neighbors but not hydrogen bonded at time t . Following previous work, we write rate equation for the decay of the two intermittent correlation functions [34]

$$\frac{-dC_{HB}(t)}{dt} = k_{HB}C_{HB}(t) - k'_{HB}N_{HB}(t), \quad (1)$$

where k_{HB} and k'_{HB} are the forward and backward rate constants, respectively. The inverse of k_{HB} can be interpreted as the average lifetime of hydrogen bonds between methanol molecules. We note that all the probability functions defined above can be calculated from simulation trajectories by calculating time correlations of appropriately constructed population variables [33–41]. Once these correlation functions are calculated, we obtained the average hydrogen bond lifetime by integrating the continuous probability function $S_{HB}(t)$ and the rate constants through least square fit of simulated results of $C_{HB}(t)$ and $N_{HB}(t)$ to Eq. (1) in the short time ($0 < t < 4$ ps) and long-time ($4 < t < 12$ ps) regions. The forward rate constants obtained through such fits are denoted as $k_{HB,short}$ and $k_{HB,long}$, respectively.

The relaxation of hydrogen bond correlation functions is shown in Fig. 3 at both temperatures of 300 and 350 K and the corresponding relaxation times are included in Table I. As expected, the relaxation is found to be faster at the higher temperature. The value of τ_{HB} is found to be 1.85 ps at 300 K and 0.92 ps at 350 K. We note that these values are for BLYP functional with dispersion corrections. The corresponding result for pure BLYP without any dispersion corrections was found to be 2.8 ps in a recent study [1] and the experimental time scale as reported in Ref. [4] is 1.6 ± 0.3 ps. Thus, the dispersion corrections make the dynamics faster which is in better agreement with experiments [4]. The route of intermittent correlations provide the following values of the inverse rate constants at short times: 2.0 ps at 300 K and 0.81 ps at 350 K. The corresponding long-time results are: 5.67 ps at 300 K and 5.56 ps at 350 K. The short time results are similar to the values of τ_{HB} obtained from the route of continuous correlation function which is expected because both $S_{HB}(t)$ and the short time part of $C_{HB}(t)$ capture the hydrogen bond breaking and making dynamics due to fast librational, rotational and short time translational motion. Henceforth, this time constant of ~ 1.8 ps at 300 K and 0.9 ps at 350 K

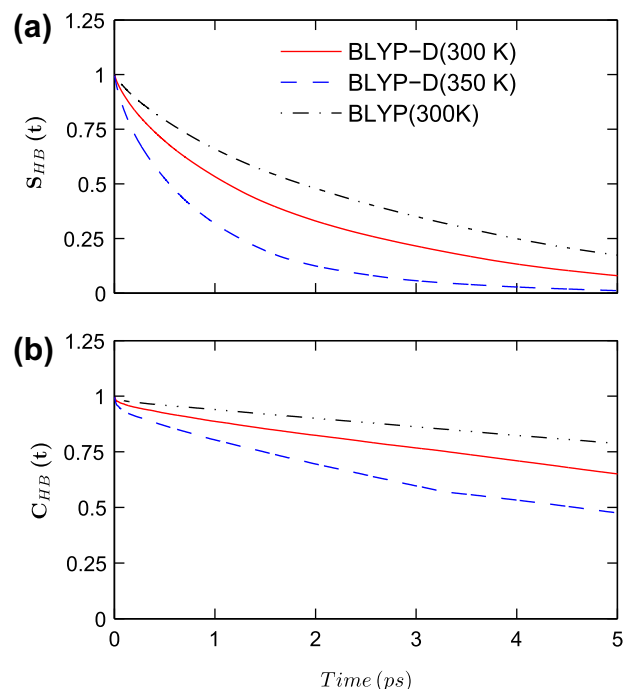


Fig. 3. The time dependence of the (a) continuous and (b) intermittent hydrogen bond time correlation functions. The solid and dashed curves represent the BLYP-D results at 300 and 350 K. The corresponding results for BLYP functional without dispersion corrections at 300 K (Ref.1) are shown by dashed-dotted curves.

Table I

Values of various time constants (ps) of hydrogen bond dynamics in liquid methanol. The BLYP results are taken from Ref. [1].

Functional	Temperature	τ_{HB}	$1/k_{HB,short}$	$1/k_{HB,long}$
BLYP-D	300	1.85	2.03	5.56
BLYP-D	350	0.92	0.81	5.67
BLYP	300	2.80	2.52	15.06

will be referred to as the hydrogen bond lifetimes at these temperatures. The long time decay actually corresponds to the escape dynamics or slow diffusion of methanol molecules from their initial solvation shells [1].

Next, we focus on the dynamics of vibrational frequency fluctuations or the so-called vibrational spectral diffusion. The dynamics of frequency fluctuations can be described through the decay of the the frequency time correlation function defined as [3,5,6,42–44]

$$C_{\omega}(t) = \langle \delta\omega(t)\delta\omega(0) \rangle / \langle \delta\omega(0)^2 \rangle, \quad (2)$$

where $\delta\omega(t)$ stands for the frequency fluctuation of an OD bond at time t from its average frequency. The average is taken over the initial time and over all the OD groups present in the system. The results for both the systems are shown in Fig. 4. A fast decay at 200 fs shows the short time part of the dynamics which is then followed by a slow decay extending up to a few ps for all the systems. Also, the dynamics of frequency fluctuations is found to be somewhat faster for the BLYP-D functional than that for the BLYP functional at 300 K.

We have used the following tri-exponential fitting function

$$f(t) = a_0 \cos \omega_s t e^{-\frac{t}{\tau_0}} + a_1 e^{-\frac{t}{\tau_1}} + (1 - a_0 - a_1) e^{-\frac{t}{\tau_2}}, \quad (3)$$

where the first term of the fitting function takes care of the slight oscillation that is found around 100–200 fs. The values of the various terms of the above function are found to be: $\omega_s = 99.58 \text{ cm}^{-1}$, $\tau_0 = 100 \text{ fs}$, $\tau_1 = 160 \text{ fs}$ and $\tau_2 = 2.15 \text{ ps}$ at 300 K. The corresponding values for the system at 350 K are found to be: $\omega_s = 99.60 \text{ cm}^{-1}$, $\tau_0 = 100 \text{ fs}$, $\tau_1 = 80 \text{ fs}$ and $\tau_2 = 1.14 \text{ ps}$. Details of the various relaxation times, frequency and weights are given in Tables II and III. The oscillation in the short time region is likely due to the underdamped motion of the intact hydrogen bonded O–O pairs [1,5,6].

Another way of investigating the spectral diffusion is to look at the dynamics of a hole that is created by selective removal of particular OD frequencies in the different frequency regions of the inhomogeneous equilibrium distribution. We assume that a

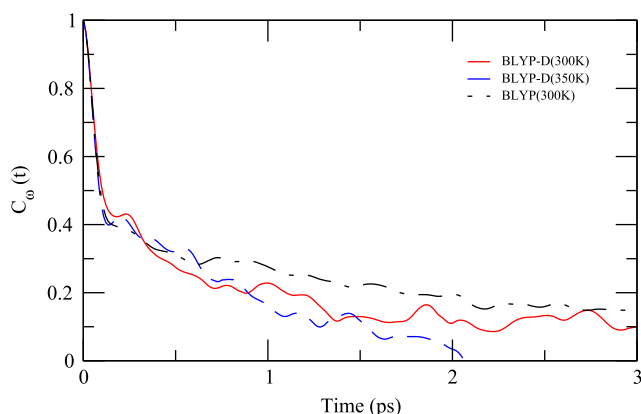


Fig. 4. The time correlation function of OD fluctuating frequencies averaged over all the molecules of the system. The solid and dashed curves represent the BLYP-D results at 300 and 350 K. The corresponding results for BLYP functional without dispersion corrections at 300 K (Ref.1) are shown by dashed-dotted curves.

Table II

Values of various time Constants (ps), frequency (cm^{-1}), and weights of the dynamics of vibrational spectral diffusion in liquid methanol at 300 K obtained with the dispersion corrected BLYP-D functional. The quantities in brackets in the fifth column are the corresponding time scales obtained with the BLYP functional in Ref. [1].

Quantity	Excitation	τ_0	τ_1	τ_2	ω_s	a_0	a_1
$C_{\omega}(t)$	–	0.10	0.16	2.15 (3.1)	99.58	0.27	0.42
$\Delta\bar{\omega}_b(t)$	blue	0.14	0.12	1.8 (3.0)	112.5	0.21	0.45
$\Delta\bar{\omega}_r(t)$	blue	0.13	0.14	3.3 (6.0)	111.2	0.23	0.43
$\Delta\bar{\omega}_b(t)$	red	0.19	0.13	2.8 (5.9)	110.0	0.14	0.46
$\Delta\bar{\omega}_r(t)$	red	0.20	0.10	1.7 (3.4)	111.1	0.12	0.45

Table III

Values of various time Constants (ps), frequency (cm^{-1}), and weights of the dynamics of vibrational spectral diffusion in liquid methanol at 350 K obtained with the dispersion corrected BLYP-D functional.

Quantity	Excitation	τ_0	τ_1	τ_2	ω_s	a_0	a_1
$C_{\omega}(t)$	–	0.10	0.08	1.14	99.6	0.28	0.10
$\Delta\bar{\omega}_b(t)$	blue	0.19	0.11	1.2	113.8	0.10	0.37
$\Delta\bar{\omega}_r(t)$	blue	0.10	0.34	2.9	78.36	0.25	0.30
$\Delta\bar{\omega}_b(t)$	red	0.11	0.23	2.8	116.3	0.23	0.37
$\Delta\bar{\omega}_r(t)$	red	0.15	0.12	1.3	111.2	0.17	0.40

Gaussian frequency hole of the following form is created at the initial time $t = 0$ [5,6,43,44]

$$P_h(\omega, 0) = P_{eq}(\omega) e^{-\frac{(\omega - \omega_p)^2}{2\sigma^2}}, \quad (4)$$

where ω_p denotes the pulse center frequency and $P_{eq}(\omega)$ denotes the equilibrium distribution of all the OD frequencies present in the system. The value of σ is taken to be 70 cm^{-1} . The initial distribution of the remaining frequencies is equal to $P_{eq}(\omega) - P_h(\omega, 0)$. We note that the time evolution of this initially created non-equilibrium distribution is closely related to pump–probe signals of the time dependent infrared spectroscopic experiments. We have calculated the time evolution of the nonequilibrium distribution $P_r(\omega, t)$ and $P_h(\omega, t)$ for large set of system trajectories reflecting the initial distribution $P_r(\omega, 0)$ and $P_h(\omega, 0)$, respectively, and, from these time dependent probability distributions, the average frequencies of the hole and remaining modes are calculated.

We created the hole in two different frequency regions: One centered at the red side at $\omega_p = \bar{\omega} - 100 \text{ cm}^{-1}$ and the other one is centered at the blue side at $\omega_p = \bar{\omega} + 100 \text{ cm}^{-1}$ where $\bar{\omega}$ is the average frequency of all the OD modes of methanol present in the system. In Figs. 5 and 6, we have shown the time evolution of the hole and remaining distributions after creation of the hole at $t = 0$. In these figures, the results are shown for both temperatures of 300 and 350 K. The frequency is expressed in terms shift ($\Delta\omega$) from its equilibrium value. As soon as hole is created in the blue region, it starts shifting toward the red region until it becomes symmetric around the equilibrium value. Similarly, the remaining distribution shifts toward the blue side with time and the hole in the blue region is filled gradually and finally the distribution adopts a symmetric shape around $\bar{\omega}$, that is around $\Delta\omega = 0$. An opposite behavior is found when the hole is created in the red region.

In Fig. 7, the average frequencies of the hole modes for blue as well as red excitations are shown at 300 and 350 K and the corresponding values for the remaining modes are shown in Fig. 8. From these figures, we obtain the time scales of relaxation by fitting to a function of similar form as in Eq. (3). Here also, it is found that there is a fast decay followed by an oscillation and thereafter a slower decay follows that extends up to few ps. It is interesting to note that the oscillations for the lower frequency modes are more pronounced such as the remaining modes for blue and red

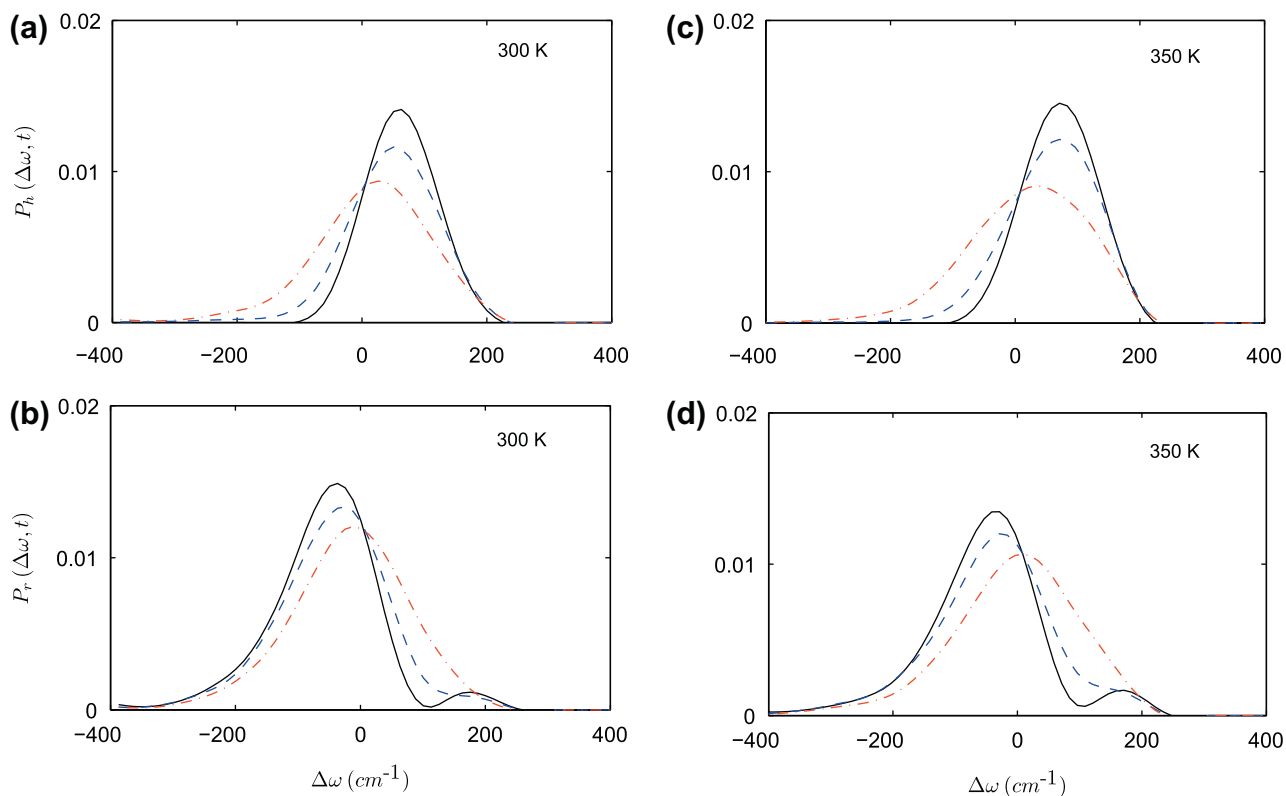


Fig. 5. The time variation of the distribution of (a,c) hole and (b,d) remaining modes after hole creation in the blue at time $t = 0$. The solid, dashed and dashed-dotted curves represent the calculated results for times $t = 10$ fs, 50 fs and 1.25 ps obtained with the BLYP-D functional.

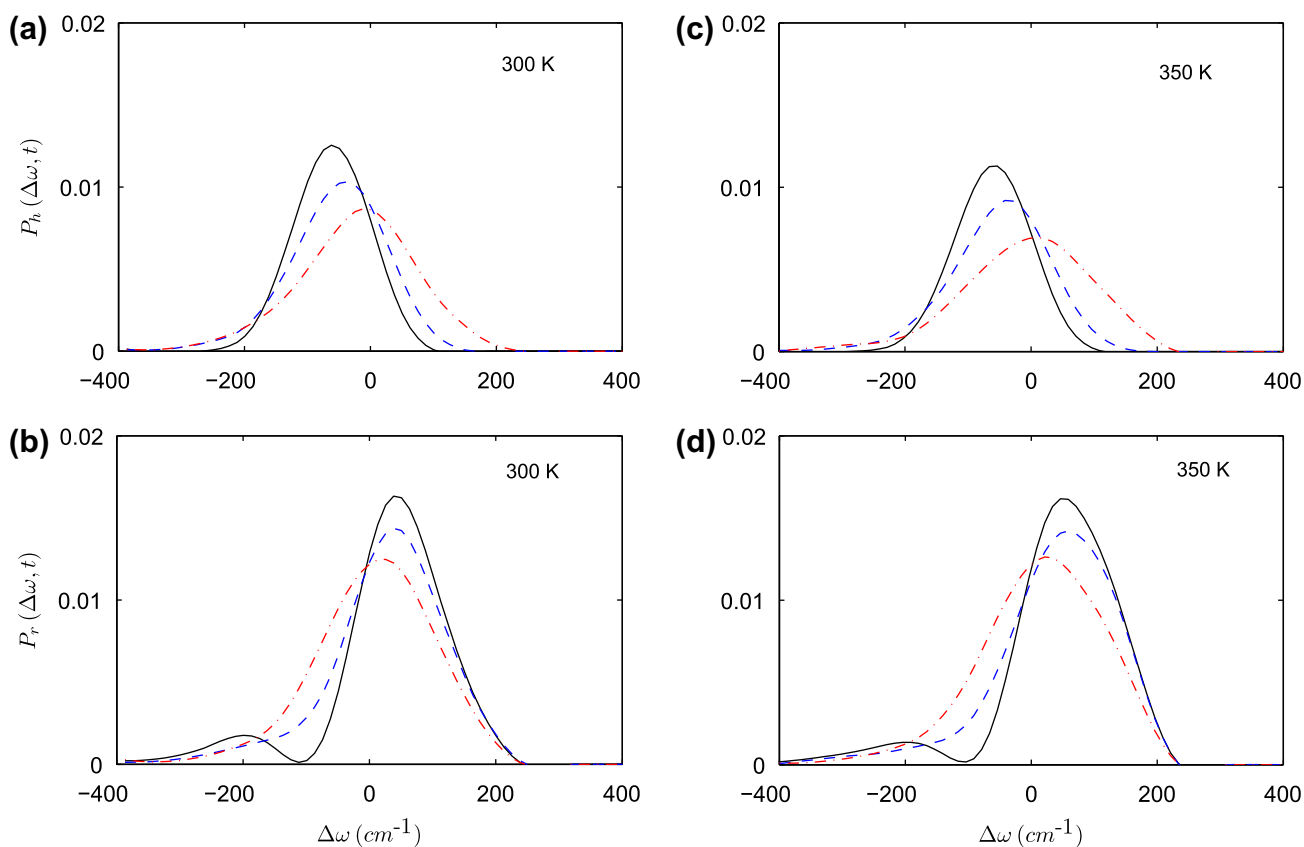


Fig. 6. The time variation of the distribution of (a,c) hole and (b,d) remaining modes after hole creation in the red at time $t = 0$. The solid, dashed and dashed-dotted curves represent the calculated results for times of 10 fs, 50 fs and 1.25 ps obtained with the BLYP-D functional.

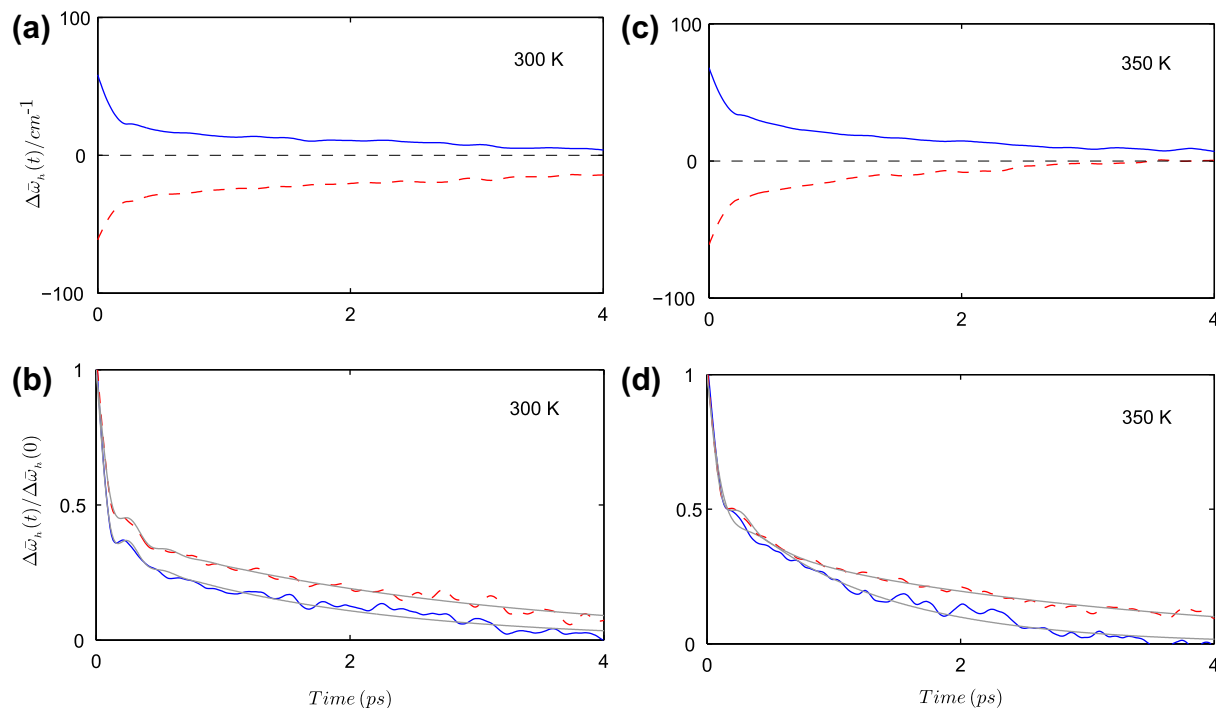


Fig. 7. The time variation of the (a,c) average frequency shifts of the hole modes after hole creation in the blue and red sides of the average frequency. The corresponding results after normalization by the initial frequency shifts are shown in (b,d). In all the figures, the solid and dashed curves correspond to hole creation in blue and red, respectively. The grey solid curves in (b) and (d) represent the fits by a function of Eq. 3 to the simulation results.

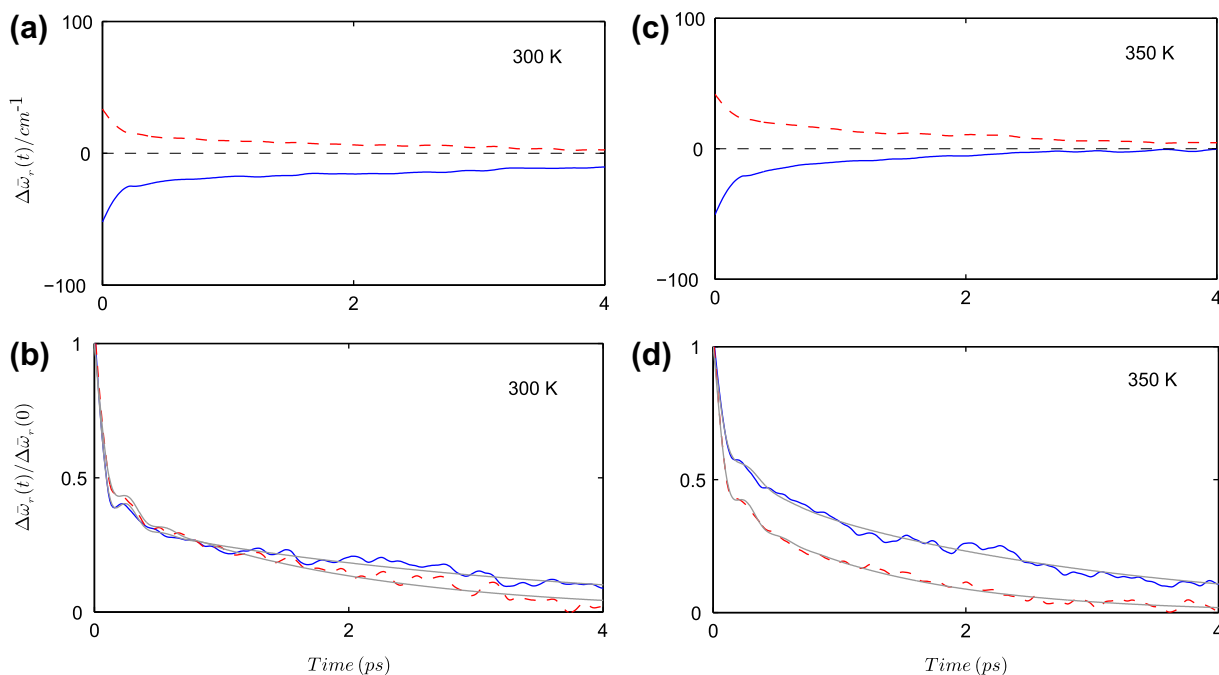


Fig. 8. The time variation of the (a,c) average frequency shifts of the remaining modes after hole creation in the blue and red sides of the average frequency. The corresponding results after normalization by the initial frequency shifts are shown in (b,d). In all the figures, the solid and dashed curves correspond to the hole creation in blue and red, respectively. The grey solid curves in (b) and (d) represent the fits by a function of Eq. 3 to the simulation results. (For interpretation of the references to colour in this figure legend, the reader is referred to the web version of this article.)

modes for hole excitations. This occurs due to involvement of the strongly hydrogen bonded OD modes which are the lower frequency modes and it shows that the oscillation in the frequency evolution comes from the under-damped intermolecular vibrations of hydrogen-bonded pairs of methanol molecules. Values of

100–150 fs and 1.7–3.0 ps are found for the fast and slow time constants of spectral diffusion at 300 K for the BLYP-D functional. The corresponding time scales at 350 K are found to be 80–100 fs and 0.9–1.2 ps, respectively. The details of various time constants for both the systems simulated with BLYP-D functional are given in

Tables II and III. The results for the BLYP functional at 300 K [1] are also included in Table II for comparison. Like the dynamics of frequency time correlations, here also the longer time scales can be attributed to the breaking dynamics of hydrogen bonds, i.e. to the hydrogen bond lifetimes.

5. Summary and conclusion

We have presented a first principles theoretical study of the effects of dispersion interactions on the dynamics of methanol molecules at two different temperatures. Specifically, we have looked at the dynamics of hydrogen bond fluctuations and vibrational spectral diffusion of methanol molecules in the liquid phase at 300 and 350 K. Some of the structural aspects of the liquid such as radial distribution functions and frequency-structure correlations have also been investigated which help to understand the dynamical aspects of this liquid. It is found that inclusion of dispersion interactions slightly increases the number of molecules held through non-hydrogen-bonded dispersion interactions at the boundary of the neighborhood which, in turn, accelerates the dynamics. The vibrational frequency of deuterated hydroxyl groups of methanol molecules is found to increase on average with the hydrogen bond distance. Our dynamical calculations are based on the so-called population correlation function approach for hydrogen bond fluctuations and a time series analysis for frequency fluctuations. The dynamics of frequency fluctuations are subsequently investigated through calculations of frequency time correlations and spectral hole dynamics calculations. It is found that inclusion of dispersion corrections makes the hydrogen bond dynamics faster compared to the case where no such dispersion corrections were included [1]. Also, the time scale of spectral diffusion obtained with dispersion corrected density functional is found to be in better agreement with experiments at room temperature [4].

Acknowledgment

Financial supports from the Department of Science and Technology (DST) and Council of Scientific and Industrial Research (CSIR), Government of India are gratefully acknowledged. Part of the calculations was done at the DST-supported High Performance Computing Facility at Computer Centre, IIT Kanpur.

References

- [1] V.K. Yadav, A. Karmakar, J. Roy Choudhuri, A. Chandra, *Chem. Phys.* 408 (2012) 36.
- [2] A.D. Becke, *Phys. Rev. A* 38 (1988) 3098; C. Lee, W. Yang, R.G. Parr, *Phys. Rev. B* 37 (1988) 785.
- [3] H.J. Bakker, J.L. Skinner, *Chem. Rev.* 110 (2010) 1498 (See, for example, for a recent review on vibrational spectral diffusion in hydrogen bonded liquids.).
- [4] I.R. Piletic, K.J. Gaffney, M.D. Fayer, *J. Chem. Phys.* 119 (2003) 423.
- [5] B.S. Mallik, A. Semparathi, A. Chandra, *J. Phys. Chem. A* 112 (2008) 5104.
- [6] B.S. Mallik, A. Semparathi, A. Chandra, *J. Chem. Phys.* 129 (2008) 194512.
- [7] M. Sprik, J. Hutter, M. Parrinello, *J. Chem. Phys.* 105 (1996) 1142.
- [8] J. VandeVondele, F. Mohamed, M. Krack, J. Hutter, M. Sprik, M. Parrinello, *J. Chem. Phys.* 122 (2005) 014515.
- [9] I.-F.W. Kuo, C.J. Mundy, M.J. McGrath, J.I. Siepmann, J. VandeVondele, M. Sprik, J. Hutter, B. Chen, M.L. Klein, F. Mohamed, M. Krack, M. Parrinello, *J. Phys. Chem. B* 108 (2004) 12990.
- [10] P.H.-L. Sit, N. Marzari, *J. Chem. Phys.* 122 (2005) 204510.
- [11] A. Chandra, M. Tuckerman, D. Marx, *Phys. Rev. Lett.* 99 (2007) 145901.
- [12] H.-S. Lee, M.E. Tuckerman, *J. Chem. Phys.* 126 (2007) 164501.
- [13] S. Yoo, X.C. Zeng, S.S. Xantheas, *J. Chem. Phys.* 130 (2009) 221102.
- [14] D. Chakraborty, A. Chandra, *Chem. Phys.* 392 (2012) 96.
- [15] R. Jonchiere, A.P. Seitsonen, G. Ferlat, A.M. Saitta, R. Vuilleumier, *J. Chem. Phys.* 135 (2011) 154503.
- [16] J. Wang, G. Roman-Perez, J.M. Soler, E. Artacho, M.-V. Fernandez-Serra, *J. Chem. Phys.* 134 (2011) 024516.
- [17] S. Yoo, S.S. Xantheas, *J. Chem. Phys.* 134 (2011) 121105.
- [18] J. Schmidt, J. VandeVondele, I.-F.W. Kuo, D. Sebastiani, J.I. Siepmann, J. Hutter, C.J. Mundy, *J. Phys. Chem. B* 113 (2009) 11959.
- [19] M.J. McGrath, I.-F.W. Kuo, J.I. Siepmann, *Phys. Chem. Chem. Phys.* 13 (2011) 19943.
- [20] M.J. McGrath, I.-F.W. Kuo, J.N. Ghogomu, C.J. Mundy, J.I. Siepmann, *J. Phys. Chem. B* 115 (2011) 11688.
- [21] S. Grimme, *J. Comput. Chem.* 25 (2004) 1463; *J. Comput. Chem.* 27 (2006) 1787.
- [22] S. Grimme, J. Antony, T. Schwabe, C. Mück-Lichtenfeld, *Org. Biomol. Chem.* 5 (2007) 741.
- [23] R. Car, M. Parrinello, *Phys. Rev. Lett.* 55 (1985) 2471.
- [24] L.V. Vela-Arevalo, S. Wiggins, *Int. J. Bifur. Chaos* 11 (2001) 1359.
- [25] D. Marx, J. Hutter, *Ab Initio Molecular Dynamics: Basic Theory and Advanced Methods*, Cambridge University Press, Cambridge, 2009.
- [26] J. Hutter, A. Alavi, T. Deutsch, M. Bernasconi, S. Goedecker, D. Marx, M. Tuckerman, M. Parrinello, CPMD Program MPI Fur Festkörperforschung and IBM Zurich Research Laboratory.
- [27] D.R. Lide (Ed.), *Handbook of Chemistry and Physics*, 87, CRC, FL/Taylor and Francis, Boca Raton, London, 2006.
- [28] W. Kohn, L.J. Sham, *Phys. Rev. A* 140 (1965) 1133.
- [29] N. Troullier, J.L. Martins, *Phys. Rev. B* 43 (1991) 1993.
- [30] S. Pratihari, A. Chandra, *J. Phys. Chem. A* 114 (2010) 11869.
- [31] R. Gupta, A. Chandra, *J. Mol. Liq.* 165 (2012) 1.
- [32] D. Chakraborty, A. Chandra, *J. Chem. Phys.* 135 (2011) 114510.
- [33] D. Rapaport, *Mol. Phys.* 50 (1983) 1151.
- [34] A. Luzar, D. Chandler, *Phys. Rev. Lett.* 76 (1996) 928; A. Luzar, D. Chandler, *Nature* 53 (1996) 379 (London).
- [35] A. Luzar, *J. Chem. Phys.* 113 (2000) 10663.
- [36] A. Chandra, *Phys. Rev. Lett.* 85 (2000) 768.
- [37] S. Balasubramanian, S. Pal, B. Bagchi, *Phys. Rev. Lett.* 89 (2002) 115505.
- [38] H. Xu, H.A. Stern, *J. Phys. Chem. B* 105 (2001) 11929; H. Xu, H.A. Stern, B.J. Berne, *J. Phys. Chem. B* 106 (2002) 2054.
- [39] S. Paul, A. Chandra, *J. Chem. Phys.* 123 (2005) 184706.
- [40] S.K. Pattanayak, S. Chowdhuri, *J. Phys. Chem. B* 115 (2011) 13241.
- [41] J. Chanda, S. Bandyopadhyay, *J. Chem. Theory Comput.* 1 (2005) 963; J. Chanda, S. Bandyopadhyay, *J. Phys. Chem.* 110 (2006) 23482.
- [42] C.P. Lawrence, J.L. Skinner, *Chem. Phys. Lett.* 369 (2003) 472; C.P. Lawrence, J.L. Skinner, *J. Chem. Phys.* 117 (2003) 8847; C.P. Lawrence, J.L. Skinner, *J. Chem. Phys.* 118 (2003) 264.
- [43] R. Rey, K.B. Moller, J.T. Hynes, *J. Phys. Chem. A* 106 (2002) 11993; K.B. Moller, R. Rey, J.T. Hynes, *J. Phys. Chem. A* 108 (2004) 1275.
- [44] B.S. Mallik, A. Chandra, *J. Phys. Chem. A* 112 (2008) 13518.